Selection of Twisted Scroll Waves in Three-Dimensional Excitable Media

Daniel Margerit* and Dwight Barkley†

Mathematics Institute, University of Warwick, Coventry CV4 7AL, United Kingdom

(Received 10 April 2000)

The selection of shape and rotation frequency for scroll waves in reaction-diffusion equations modeling excitable media is investigated. For scrolls with uniform twist about straight filaments, asymptotic methods are used to derive free-boundary equations at leading and first order. Both orders are validated against full solutions of the reaction-diffusion equations. Using these two orders and with no adjustable parameters, the shape and frequency of waves are correctly predicted except possibly near the point of propagation failure where the core becomes large.

DOI: 10.1103/PhysRevLett.86.175 PACS numbers: 82.40.Ck, 47.54.+r, 87.10.+e

In three space dimensions, persistent waves in excitable media frequently take the form of scrolls which rotate about one-dimensional filaments. Figure 1 illustrates such a wave from numerical computations—the scroll is uniformly twisted along a straight filament [1]. Scroll waves of various complexities are observed in excitable chemical systems [2] and in cardiac tissue where these waves are believed responsible for certain cardiac arrhythmias [3]. The pervasiveness of these structures and their ultimate importance to biophysical and medical problems have led to considerable efforts to understand their dynamics [1,2,4], both at the fundamental level of spatiotemporal pattern formation and at a practical level specific to cardiology [3]. This Letter is aimed at the nonlinear pattern selection problem for which we derive equations predicting the shape and rotation frequency of twisted scroll waves such as in Fig. 1.

Consider the following partial-differential-equation (PDE) model of excitable media [5] written in the space-time scales proposed by Fife [6,7]:

$$\epsilon^2 \partial u/\partial t = \epsilon^2 \nabla^2 u + u(1-u)\left(u - \frac{v+b}{a}\right), \quad (1a)$$

$$\partial v/\partial t = \epsilon(u - v). \quad (1b)$$

This and similar two-component reaction-diffusion models capture essential properties of excitable media and are widely used in theoretical studies, e.g., [8–13]. Parameters a and b collectively control the excitation threshold and duration. The parameter ϵ is small, reflecting the disparate time scales of the fast activator variable u and slow inhibitor variable v.

Previous work on the selection of waves in excitable media through asymptotic expansions [9–12,14] has focused primarily on two dimensions (2D) and entirely on leading order in the small parameter ϵ. For example, expanding the rotation frequency as

$$\omega = \omega^{(0)} + \epsilon\omega^{(1)} + \cdots, \quad (2)$$

only the leading-order frequency $\omega^{(0)}$ has been obtained [10,11]. While the small-ϵ (Fife) limit has played a pivotal role in 2D theoretical studies, infinitesimal values of ϵ are not physically realized and the leading order does not accurately predict many properties of waves at finite ϵ [15]. However, one of our significant findings (Fig. 5 below) is that expansions to *first order* in ϵ are predictive well into regimes of physical interest. In this Letter we establish equations to first order in ϵ which precisely characterize the dependence of scroll shape and rotation frequency on twist and on model parameters.

For the leading-order asymptotics, we consider first the general three-dimensional (3D) case. At this order the approach is similar to that in 2D apart from an added geometrical complexity. The medium is divided into three regions: outer, interface, and core as in Fig. 2. The filament is the curve $\mathbf{X}(s,t)$ inside the core.

The outer region comprises the bulk of the medium. It consists of both excited (+) and quiescent (−) portions for which $u = u^+ = 1$ and $u = u^- = 0$, respectively, to all orders in ϵ. Expansion of the v field in the outer region gives $v = v^s + \epsilon v^{(1)} + \cdots$, where v^s is the stall concentration (value such that a plane interface is stationary) and $v^{(1)}$ is to be determined.

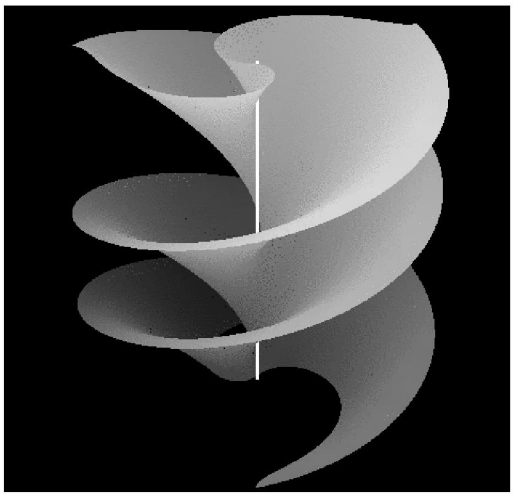

FIG. 1. Twisted scroll-wave solution of Eqs. (1). Isosurface is shown for $u = 0.5$. The filament is white. The structure rotates in time with frequency ω about the filament. The twist, defined later in the text, is $\tilde{\tau} = 0.4$ (or $\tau \approx 0.35$); $a = 1.0$, $b = 0.1$, and $\epsilon = 0.2$.

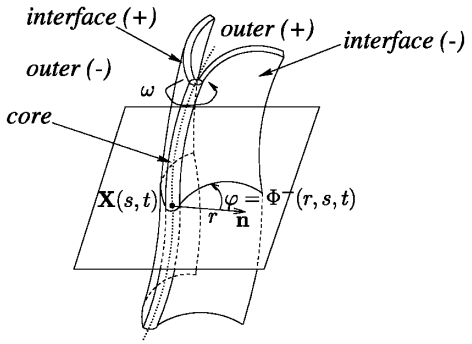

FIG. 2. Scroll geometry showing outer regions [excited (+) and quiescent (−)], interface regions [wave front (+) and wave back (−)], and core region. The filament $\mathbf{X}(s,t)$ is parametrized by s and time t. Local coordinates to the filament are (r,φ,s), with (r,φ) in the plane normal to $\mathbf{X}(s,t)$ and φ measured from $\mathbf{n}$, the normal vector to $\mathbf{X}(s,t)$.

Separating excited and quiescent states are the thin interfaces where u undergoes rapid change. These consist of a wave front (+) and a wave back (−), which on the outer scale are given by $\Phi^{\pm}(r,s,t)$. Solving leading- and first-order inner equations for u across the interface (v is constant at these orders across the interface) and matching to the outer u solution, one obtains equations for interface motion [16]. Thus Eqs. (1) reduce to equations for $v^{(1)}$ in the outer region together with equations for the motion of the two interfaces (free boundaries):

$$\partial v^{(1)}/\partial t = u^{\pm} - v^{s}, \tag{3}$$

$$-\frac{r\dot{\Phi}^{(0)\pm}h^{\pm}}{\sqrt{m^{\pm}}} = 2H^{\pm} \pm \frac{\sqrt{2}}{a}\, v^{(1)\pm}, \tag{4}$$

where $\Phi^{(0)\pm}$ is the leading-order approximation to $\Phi^{\pm}$, and where $h^{\pm} \equiv |\partial\mathbf{X}/\partial s|\,(1 - rK\cos\Phi^{(0)\pm})$, K is the filament curvature, $m^{\pm}$ is the determinant of the metric tensor, $H^{\pm}$ is the mean curvature of interface $\Phi^{(0)\pm}$, and, finally, $v^{(1)\pm}$ is the value of $v^{(1)}$ at interface $\Phi^{(0)\pm}$. Equation (4) equates normal velocity of the interface to twice the mean curvature plus the speed of a plane interface. Phenomenological approaches to excitable media yield similar equations [17].

As for spiral waves in 2D [12], the core plays no role at leading order in the solutions we consider other than to regularize the cusp that would otherwise exist as the two interfaces come together.

We consider the specific case of a straight filament and seek solutions with uniform twist $\tau \equiv \partial\Phi/\partial s$ and constant frequency $\omega^{(0)} = \dot{\Phi}^{(0)}$. The angle between the two interfaces can be shown to be constant: $\Delta\Phi^{(0)} \equiv \Phi^{(0)-} - \Phi^{(0)+} = 2\pi(1 - v^{s})$ and $v^{(1)\pm}$ can be eliminated from the free-boundary equations to obtain a single universal equation describing the shape of the interface [16]:

$$q\,\frac{d\Psi^{(0)}}{d\tilde{r}} + \frac{\Psi^{(0)}(1 + \Psi^{(0)2})}{\tilde{r}} = \tilde{r}(q + \Psi^{(0)2}) - B(q + \Psi^{(0)2})^{3/2}, \tag{5}$$

where $\Psi^{(0)} \equiv rd\Phi^{(0)+}/dr = rd\Phi^{(0)-}/dr$, and $q \equiv 1 + \tilde{\tau}^2\tilde{r}^2$, with $\tilde{r} = \sqrt{\omega^{(0)}}r$, $\tilde{\tau} = \tau/\sqrt{\omega^{(0)}}$. The eigenvalue B is related to $\omega^{(0)}$ and model parameters via

$$B = (\mu/\omega^{(0)})^{3/2}, \qquad \mu^{3/2} = \sqrt{2}\,\pi v^{s}(1 - v^{s})/a\,, \tag{6}$$

where $v^{s} = a/2 - b$. With $\tilde{\tau} = 0$, Eq. (5) is as given by Karma [11] with Eq. (6) giving the leading-order spiral frequency $\omega^{(0)}$ as a function of parameters (a,b). For $\tilde{\tau} \neq 0$, Eq. (5) agrees with the work of Bernoff [10].

Figure 3(a) shows $\Psi^{(0)}$ at two values of $\tilde{\tau}$ and Fig. 4(a) shows dependence of the selected B as a function of τ^2/μ [19]. These results are obtained by shooting: integrating Eq. (5) from $\tilde{r} = 0$ to large $\tilde{r}$ and finding B such that $\Psi^{(0)}$ matches the relevant large-$\tilde{r}$ limit from Eq. (5):

$$\Psi^{(0)}(\tilde{r} \to \infty) = -\frac{\tilde{r}}{B}\sqrt{1 - B^2\tilde{\tau}^2} - \frac{1}{B^2} + O\left(\frac{1}{\tilde{r}}\right). \tag{7}$$

We turn to the order-ϵ asymptotics. For a straight scroll with twist τ rotating at frequency ω, we have $\partial/\partial t = -\omega\partial/\partial\varphi$ and $\partial/\partial z = \tau\partial/\partial\varphi$. For this case Eqs. (1) become

$$-\epsilon^2\omega\,\partial u/\partial\varphi = \epsilon^2\nabla_{\perp}^2 u + u(1 - u)\left(u - \frac{v + b}{a}\right), \tag{8a}$$

$$-\omega\,\partial v/\partial\varphi = \epsilon(u - v)\,, \tag{8b}$$

where $\nabla_{\perp}^2 = \partial^2/\partial r^2 + (1/r)\partial/\partial r + (q/r^2)\partial^2/\partial\varphi^2$. From (8), solving leading-, first-, and second-order inner equations for u and v across the interface (v is not a constant across the interface at second order) and matching to the solution in the outer region at these orders, one obtains [16] $\Delta\Phi^{(1)} \equiv \Phi^{(1)-} - \Phi^{(1)+} = 0$ and one again obtains a single universal equation for the interface shape:

$$q\,\frac{d\Psi^{(1)}}{d\tilde{r}} + l(\tilde{r})\Psi^{(1)} = m(\tilde{r}) = Dm_1(\tilde{r}) + m_2(\tilde{r})\,, \tag{9}$$

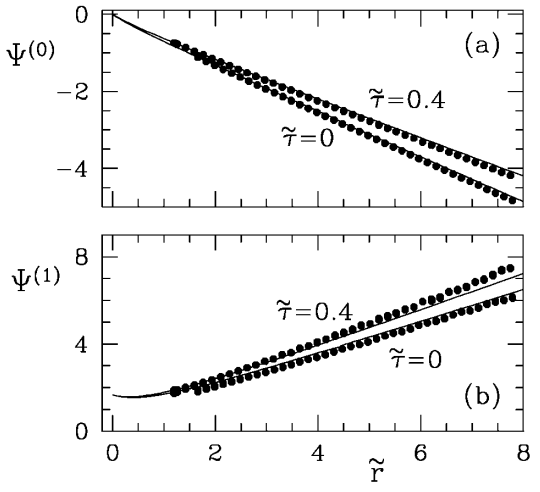

FIG. 3. Shape functions Ψ at leading order (a) and first order (b) for two values of $\tilde{\tau}$: $\tilde{\tau} = 0$ corresponds to 2D spiral waves and $\tilde{\tau} = 0.4$ is the case shown in Fig. 1 [18]. Curves are free-boundary solutions; points are from PDE solutions.

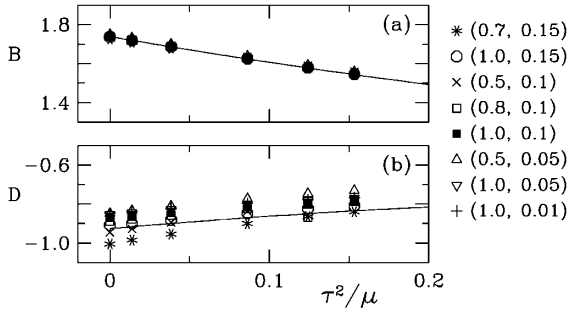

FIG. 4. Dependence of eigenvalues B and D on twist. Curves are free-boundary solutions; points are from PDE solutions for values of (a, b) given in the legend.

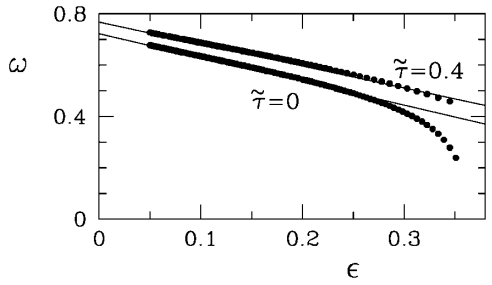

FIG. 5. Scroll frequency ω versus ϵ from numerical solutions of PDE (8) for two values of twist. Lines are fits to the data at small ϵ and are indistinguishable from asymptotic predictions at first order in ϵ. $(a, b) = (1.0, 0.1)$.

where $\Psi^{(1)} \equiv a\omega^{(0)} r d\Phi^{(1)\pm}/dr$ and

$$l(\tilde{r}) = \frac{1}{\tilde{r}} + \tilde{r}\Psi^{(0)} + 3\Psi^{(0)}\left[\frac{\Psi^{(0)}}{\tilde{r}} - \tilde{r} + B\sqrt{q + \Psi^{(0)2}}\right],$$

$$m_1(\tilde{r}) = \tilde{r}(q + \Psi^{(0)2}) + B(q + \Psi^{(0)2})^{3/2},$$

$$m_2(\tilde{r}) = \frac{5}{3}\frac{(q + \Psi^{(0)2})^2}{\tilde{r}}.$$

The eigenvalue D in Eq. (9) is related to $\omega^{(1)}$ by

$$D = a\omega^{(1)}. \tag{10}$$

The large-$\tilde{r}$ behavior of $\Psi^{(1)}$ is

$$\Psi^{(1)}(\tilde{r} \to \infty) = -\left(2D + \frac{5}{3}\frac{1}{B^2}\right)\frac{\tilde{r}}{B\sqrt{1 - \tilde{\tau}^2 B^2}} - \frac{5 + 3DB^2}{B^4} + O\left(\frac{1}{\tilde{r}}\right). \tag{11}$$

The general solution of Eq. (9) is

$$\Psi^{(1)}(\tilde{r}) = \Psi_h^{(1)}(\tilde{r})\left(A + \int_0^{\tilde{r}} \frac{m(\rho)}{\Psi_h^{(1)}(\rho)}\, d\rho\right), \tag{12}$$

where $\Psi_h^{(1)}$ is the homogeneous solution

$$\Psi_h^{(1)} = \frac{1}{q\tilde{r}}(q + \Psi^{(0)2})^{3/2} \exp\left(-\int_0^{\tilde{r}} \frac{\rho\Psi^{(0)}(\rho)}{1 + \tilde{\tau}^2\rho^2}\, d\rho\right).$$

For $\Psi^{(1)}$ to be finite at $\tilde{r} \to 0$, $A \equiv 0$. Then solutions to Eq. (12) diverge exponentially at infinity unless D has the selected value

$$D = -\frac{c_2}{c_1}, \qquad c_i = \int_0^{\infty} [m_i(\rho)/\Psi_h^{(1)}(\rho)]\, d\rho. \tag{13}$$

Figure 3(b) shows solutions to Eq. (9) and Fig. 4(b) shows D from Eq. (13) as a function of twist.

We now compare the asymptotic results with full PDE solutions. For this we use Newton's method [13] to solve Eqs. (8) for twisted, straight scroll waves. The operator $\nabla_\perp^2$ is discretized on a polar grid typically with 256 points in φ and radial spacing $\Delta r = 0.05$. The r derivatives are computed by finite differences and φ derivatives are computed spectrally.

Figure 5 shows the dependence of ω on ϵ from the PDE solutions. This figure clearly shows the existence of the Fife limit: a finite-frequency limit as $\epsilon \to 0$. Over a substantial range of ϵ, the frequency is very well captured by the first two orders in ϵ: $\omega \simeq \omega^{(0)} + \epsilon\omega^{(1)}$. The linear approximation fails only near the point of propagation failure where no waves are supported by the medium [8,20]. For 2D waves ($\tilde{\tau} = 0$), ω falls to zero near this point, while the branch of twisted waves ends at finite ω.

Extrapolation of frequency data to $\epsilon = 0$ gives $\omega^{(0)}$ and thus B by Eq. (6). The slope of ω versus ϵ gives $\omega^{(1)}$ and hence D by Eq. (10). Using least-squares fits to numerical data, we have obtained B and D for parameters (a, b) spanning the values for which waves are found [13]. The results plotted in Fig. 4 compare well with asymptotic predictions. There is scatter in the values of D due to higher-order effects, small on the scale of Fig. 5.

From the computed u fields we find the functions $\Phi^{\pm}$ as curves on which $u = 1/2$ and from these Ψ is computed by differencing. Analogously to the frequency, from the dependence of Ψ on ϵ we find $\Psi^{(0)}$ [Fig. 3(a)] and $\Psi^{(1)}$ [Fig. 3(b)]. [Only the data for $(a, b) = (1.0, 0.1)$ are shown, but other cases are similar.] There is again good agreement with asymptotic predictions.

In Fig. 6 we compare full solutions of PDE (8) with the interface curves at leading order ($\varphi = \Phi^{(0)\pm}$) and at leading plus first order ($\varphi = \Phi^{(0)\pm} + \epsilon\Phi^{(1)\pm}$). With the first-order contribution, the agreement is excellent and contains *no adjustable parameters*.

The solutions we have obtained are straight scroll waves with uniform twist which rotate uniformly in time. These solutions do not exhibit unwinding, observed in finite geometries [21], in which the twist decays to zero. Solutions may be unstable to perturbations however. Direct time-dependent simulations of Eqs. (1) in 2D [5] show that the spiral wave in Fig. 6 is linearly stable. Simulations of Eqs. (1) in 3D [22] with imposed vertical periodicity over distance $2\pi/\tau$ show that at $(a, b, \epsilon) = (1.0, 0.1, 0.2)$ the straight scroll first becomes linearly unstable at $\tau \approx 0.3$ ($\tilde{\tau} \approx 0.35$). The state in Figs. 6(c) and 6(d) is thus slightly beyond the instability threshold: after many tens of rotations, the scroll undergoes transition to a helical state [1,23].

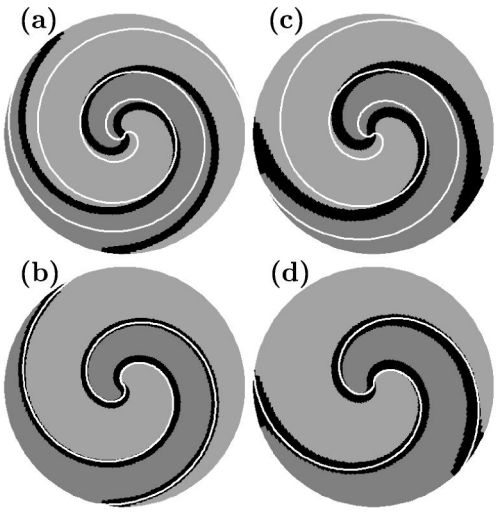

FIG. 6. Comparison between PDE solutions (grey scale) and asymptotic results (white curves). (a) $\tilde{\tau} = 0$, asymptotics at leading order. (b) $\tilde{\tau} = 0$, asymptotics at leading plus first order. (c) $\tilde{\tau} = 0.4$ ($\tau \approx 0.35$), asymptotics at leading order. (d) $\tilde{\tau} = 0.4$ ($\tau \approx 0.35$), asymptotics at leading plus first order. Black is the interface $0.1 \leq u \leq 0.9$; light grey (dark grey) is $u < 0.1$ ($u > 0.9$). The radius is 20; $a = 1.0$, $b = 0.1$, $\epsilon = 0.2$.

We summarize the significance of our results. For *any* desired model parameters (a, b, ϵ) and twist τ, the scroll frequency can be approximated as $\omega = \omega^{(0)} + \epsilon\omega^{(1)}$, where $\omega^{(0)}$ and $\omega^{(1)}$ are found from (6) and (10) with eigenvalues B and D read off from Fig. 4. In addition, the limits (7) and (11) are good approximations for $r \gtrsim 4$. Hence away from the filament the scroll shape can be obtained directly from B and D without explicitly solving for the shape functions $\Psi^{(0)}$ and $\Psi^{(1)}$. Implicitly this provides the dispersion relation—frequency as function of scroll wavelength—commonly used to characterize waves in excitable media, e.g., [15].

In conclusion, we have solved the selection problem for twisted scroll waves in excitable media with straight filaments, and we have directly validated leading-order and first-order free-boundary equations by comparison with full PDE solutions. These two orders provide excellent approximations to PDE solutions except possibly near the point of propagation failure. We have considered a specific PDE model of excitable media, but as in [10,11], the free-boundary equations we have derived apply to a large class of models. It would be of interest in the future to consider more extensively the linear stability of straight twisted solutions, to extend this analysis to more complex scroll waves where the motion of filaments is important, and finally to compare the asymptotic solutions directly with experimental results.

The work has been supported in part by the EPSRC under Grant No. GR/K88118.

*Present address: Institut de Mécanique des Fluides de Toulouse, 31400 Toulouse Cedex, France.
Email address: margerit@imft.fr
†URL: http://www.maths.warwick.ac.uk/~barkley

[1] A. T. Winfree, SIAM Rev. **32**, 1 (1990).
[2] Physica (Amsterdam) **49D**, (1991), and references therein; A. T. Winfree, Physica (Amsterdam) **84D**, 126 (1995), and references therein; in *Chemical Waves and Patterns,* edited by R. Kapral and K. Showalter (Kluwer, London, 1995), pp. 3–56, and references therein.
[3] The most recent review can be found in Chaos **8** (1998).
[4] J. P. Keener and J. J. Tyson, SIAM Rev. **34**, 1 (1992), and references therein; V. N. Biktashev, A. V. Holden, and H. Zhang, Philos. Trans. R. Soc. London A **347**, 611 (1994); M. Gabbay, E. Ott, and P. Guzdar, Phys. Rev. Lett. **78**, 2012 (1998).
[5] D. Barkley, Physica (Amsterdam) **49D**, 61 (1991).
[6] P. C. Fife, in *Non-Equilibrium Dynamics in Chemical Systems,* edited by C. Vidal and A. Pacault (Springer, New York, 1984), pp. 76–88.
[7] Reference [5] uses a different choice of scales; ϵ^3 gives the value of ϵ used in Ref. [5].
[8] A. T. Winfree, Chaos **1**, 303 (1991).
[9] J. J. Tyson and J. P. Keener, Physica (Amsterdam) **32D**, 327 (1988).
[10] A. Bernoff, Physica (Amsterdam) **53D**, 125 (1991).
[11] A. Karma, Phys. Rev. Lett. **68**, 397 (1992).
[12] D. Kessler, H. Levine, and W. Reynolds, Phys. Rev. Lett. **68**, 401 (1992); Physica (Amsterdam) **70D**, 115 (1994).
[13] D. Barkley, Phys. Rev. Lett. **72**, 164 (1994); in *Chemical Waves and Patterns,* edited by R. Kapral and K. Showalter (Kluwer, London, 1995), pp. 163–190.
[14] A phenomenological (kinematic) approach has alternatively been used, e.g., A. S. Mikhailov and V. S. Zykov, Physica (Amsterdam) **52D**, 379 (1991), and references therein.
[15] A. L. Belmonte, Q. Ouyang, and J. M. Flesselles, J. Phys. II (France) **7**, 1425 (1997).
[16] D. Margerit and D. Barkley (to be published).
[17] P. K. Brazhnik, V. A. Davydov, V. S. Zykov, and A. S. Mikhailov, Sov. Phys. JETP **66**, 984 (1987); H. Yamada and K. Nozaki, J. Phys. Soc. Jpn. **63**, 379 (1994).
[18] For $(a, b) = (1.0, 0.1)$, $\mu = 1.0437\ldots$ and $\tilde{\tau} = 0.4$ corresponds to $\tau = 0.350\,42\ldots$.
[19] While $\tilde{\tau}$ is the appropriate universal representation for twist, τ^2/μ is more useful in practice because it is directly obtainable from dimensional twist τ and model parameters via μ in Eq. (6). This representation is also universal since $\tau^2/\mu = \tilde{\tau}^2/B^{2/3}$, and $\tilde{\tau}$ and B are universal.
[20] V. Hakim and A. Karma, Phys. Rev. Lett. **79**, 665 (1997).
[21] A. M. Pertsov, R. R. Aliev, and V. I. Krinsky, Nature (London) **345**, 419 (1990).
[22] M. Dowle, R. M. Mantel, and D. Barkley, Int. J. Bifurcation Chaos **7**, 2529 (1997).
[23] C. Henze, E. Lugosi, and A. Winfree, Can. J. Phys. **68**, 683 (1990).